JACS
JOURNAL OF THE AMERICAN CHEMICAL SOCIETY
Article
pubs.acs.org/JACS

Up-Conversion Intersystem Crossing Rates in Organic Emitters for Thermally Activated Delayed Fluorescence: Impact of the Nature of Singlet vs Triplet Excited States

Pralok K. Samanta,[†] Dongwook Kim,[*,†,‡] Veaceslav Coropceanu,[§] and Jean-Luc Brédas[*,†]

[†]Laboratory for Computational and Theoretical Chemistry of Advanced Materials, Physical Science and Engineering Division, King Abdullah University of Science and Technology, Thuwal 23955-6900, Kingdom of Saudi Arabia

[‡]Department of Chemistry, Kyonggi University, 154-42 Gwanggyosan-Ro, Yeongtong-Gu, Suwon 440-760, Korea

[§]School of Chemistry and Biochemistry, Center for Organic Photonics and Electronics (COPE), Georgia Institute of Technology, Atlanta, Georgia 30332-0400, United States

Supporting Information

ABSTRACT: The rates for up-conversion intersystem crossing (UISC) from the T_1 state to the S_1 state are calculated for a series of organic emitters with an emphasis on thermally activated delayed fluorescence (TADF) materials. Both the spin−orbit coupling and the energy difference between the S_1 and T_1 states (ΔE_{ST}) are evaluated, at the density functional theory (DFT) and time-dependent DFT levels. The calculated UISC rates and ΔE_{ST} values are found to be in good agreement with available experimental data. Our results underline that small ΔE_{ST} values and sizable spin−orbit coupling matrix elements have to be simultaneously realized in order to facilitate UISC and ultimately TADF. Importantly, the spatial separation of the highest occupied and lowest unoccupied molecular orbitals of the emitter, a widely accepted strategy for the design of TADF molecules, does not necessarily lead to a sufficient reduction in ΔE_{ST}; in fact, either a significant charge-transfer (CT) contribution to the T_1 state or a minimal energy difference between the local-excitation and charge-transfer triplet states is required to achieve a small ΔE_{ST}. Also, having S_1 and T_1 states of a different nature is found to strongly enhance spin−orbit coupling, which is consistent with the El-Sayed rule for ISC rates. Overall, our results indicate that having either similar energies for the local-excitation and charge-transfer triplet states or the right balance between a substantial CT contribution to T_1 and somewhat different natures of the S_1 and T_1 states, paves the way toward UISC enhancement and thus TADF efficiency improvement.

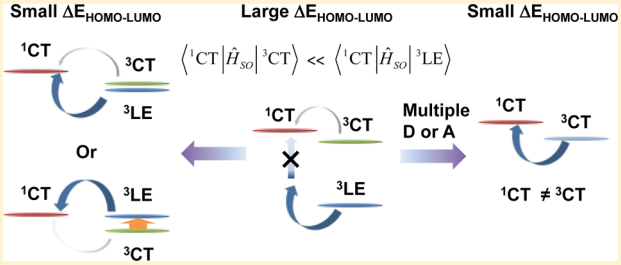

1. INTRODUCTION

Organic light-emitting diodes (OLEDs) have demonstrated their practical utility due to highly efficient electroluminescence, lightweight, mechanical flexibility, as well as possibility of solution processing and low-cost manufacture.[1−5] Devices based on vacuum processing have now entered the market of full-color flat-panel displays[6] and solid-state lighting applications.[7] In an OLED device, the light-emitting molecules are electronically excited upon recombination of charges injected from the electrodes. Since the spins of the injected charges are uncorrelated, singlet and triplet excitons are generated in a 25%:75% ratio, assuming equal efficiency of charge recombination and neglecting other processes that may affect spin statistics. In order to fabricate more efficient OLEDs, it is critical to find ways to harness the energy of the triplet excitons that represent dark states in purely organic systems. To this end, phosphorescent OLEDs have been widely studied due to their charge-to-photon internal quantum efficiency (IQE) that can reach as high as 100%[1] because of strong spin−orbit coupling (SOC) enabled by the presence of heavy metal atoms such as iridium and platinum; however, the use of these rare elements inevitably leads to high device fabrication costs.[8,9] In addition, deep-blue phosphors with long lifetimes still remain to be developed. Thus, alternatives that could be efficient in terms of light emission, cost, and chemical stability are highly desirable.

The device performance of purely organic, fluorescent OLEDs can be enhanced via a number of processes influencing spin statistics, which include triplet−triplet annihilation (TTA)[10] or exciton-polaron interaction (EPI).[11] For instance, TTA (P-type delayed fluorescence), albeit detrimental to phosphorescent OLEDs, can in principle improve the IQE of fluorescent OLEDs from 25% to 62.5%.[12] Also, in a recent report,[11] triplet-polaron interaction was suggested to generate more singlet excitons and hence to improve the performance of fluorescent OLEDs. Nevertheless, none of these processes can fully harness triplet excitons for light emission. Furthermore, both TTA and EPI are bimolecular processes and therefore more challenging to control in devices.

Received: November 24, 2016
Published: February 28, 2017

DOI: 10.1021/jacs.6b12124
J. Am. Chem. Soc. 2017, 139, 4042−4051

In contrast, although its efficiency can be influenced by the surroundings,[13,14] thermally activated delayed fluorescence (TADF) is basically a unimolecular process and can be controlled by the manipulation of the intrinsic electronic properties of the emitter. The TADF mechanism relies on an intramolecular up-conversion intersystem crossing (UISC) from a triplet excited state to a singlet excited state, which can lead to full harnessing of the triplet excitons.[15] In the systems that demonstrate UISC, we note that down-conversion ISC (DISC) from singlet to triplet excited states also occur; however, DISC competes against light emission from the singlet excited state, which re-establishes the equilibrium between singlet and triplet excited states and can eventually give rise to total depopulation of the triplet excitons provided nonradiative decay from the T_1 state is effectively suppressed.[16] Adachi et al. reported OLEDs employing 4CzIPN (2,4,5,6-tetra(9*H*-carbazol-9-yl)isophthalonitrile), a TADF material, with an IQE as high as nearly 100%.[17] Since an understanding of the relationship between UISC and TADF can allow the design of improved emitters, numerous studies have been conducted on this topic.[13,14,16,18−22]

In order to achieve efficient UISC and thus TADF, ensuring a small energy difference between the lowest singlet and lowest triplet excited states, ΔE_{ST}, is essential. In this regard, TADF molecules have often been designed following a strategy such that their highest occupied molecular orbital (HOMO) and lowest unoccupied molecular orbital (LUMO) are spatially separated (for instance, the former localized on an electron-donor moiety and the latter, on an electron-acceptor moiety) in order to minimize their wave function overlap and thereby the exchange energy, *K*. However, unless both the singlet and triplet excited states then correspond to a transition from HOMO to LUMO (which in itself carries negative implications in terms of oscillator strengths of the relevant optical transitions), this strategy is bound to fail. Indeed, for triplet excited states, in general, the larger the *K* value is, the larger their stabilization becomes[23,24] as a result, despite the spatial separation of their HOMO and LUMO wave functions, for instance, the T_1 states of many ambipolar host molecules for blue OLED applications turn out to correspond to local excitations (LE) within a particular molecular subunit rather than charge-transfer (CT) transitions from the electron donor-based HOMO to the electron acceptor-based LUMO.[25−27] Thus, having the HOMO and LUMO on separate molecular subunits is not a sufficient condition to minimize ΔE_{ST}. In addition, the spin−orbit couplings (SOC) in TADF molecules (albeit expected to be much smaller in magnitude than in heavy-metal containing phosphors) should still have significant values in order to ensure efficient UISC. To the best of our knowledge, however, studies on SOC in TADF materials are scarce.[28−30] Given the importance of UISC in TADF efficiency, systematic investigations are thus highly warranted.

Here, we report the results of our calculations on ΔE_{ST}, SOC, and UISC rate constants (k_{UISC}) for a series of representative TADF molecules: 4,5-di(9*H*-carbazol-9-yl)-phthalonitrile (2CzPN); 9,9″-(6-phenyl-1,3,5-triazine-2,4-diyl)-bis((9*H*-3,9′-bicarbazole)) (CC2TA); 12,12′-(6-([1,1′-biphenyl]-4-yl)-1,3,5-triazine-2,4-diyl)bis(11-phenyl-11,12-dihydroindolo[2,3-*a*]carbazole) (PIC-TRZ); 10-(4-(4,6-diphenyl-1,3,5-triazin-2-yl)phenyl)-10*H*-phenoxazine (PXZ-TRZ); 10-phenyl-10*H*-spiro[acridine-9,9′-fluorene]-2′,7′-dicarbonitrile (ACRFLCN); 2′,7′-bis(di-*p*-tolylamino)-9,9′-spirobi-[fluorene]-2,7-dicarbonitrile (Spiro-CN); 2,4,5,6-tetra(9*H*-carbazol-9-yl)isophthalonitrile (4CzIPN); 2,4,5,6-tetra(3,6-dimethyl-9*H*-carbazol-9-yl)isophthalonitrile (4CzIPN-Me); 3,4,5,6-tetra(9*H*-carbazol-9-yl)phthalonitrile (4CzPN); 2,3,5,6-tetra(9*H*-carbazol-9-yl)terephthalonitrile (4CzTPN), and 2,3,5,6-tetrakis(3,6-dimethyl-9*H*-carbazol-9-yl)-terephthalonitrile (4CzTPN-Me). Their chemical structures are depicted in Figure 1. For the sake of comparison, we also investigated a couple of non-TADF molecules: 4,4′-bis-(carbazol-9-yl)-*p*-biphenyl (CBP) and N,N′-diphenyl-N,N′-bis(1-naphthyl)-1,10-biphenyl-4,4′-diamine (*α*-NPD). Our discussion will underline the factors affecting ΔE_{ST} and SOC, in particular the natures of the relevant singlet and triplet excited states, as well as features that can aid in the design of more efficient TADF molecules.

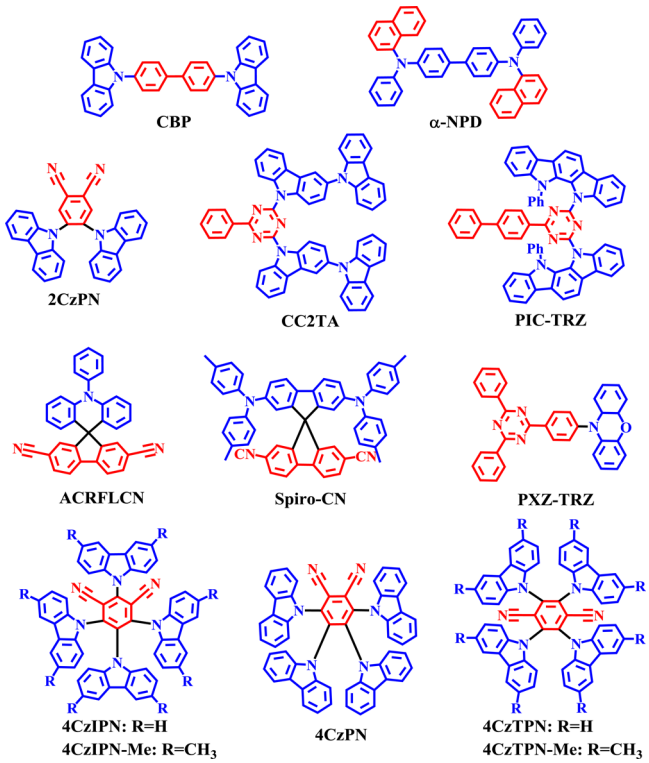

Figure 1. Chemical structures of the molecules explored in this study. The blue and red color codings denote the donor (electron-rich) and acceptor (electron-poor) molecular fragments, respectively.

2. THEORETICAL BACKGROUND AND COMPUTATIONAL DETAILS

Up-Conversion Intersystem Crossing Rate. The UISC rate constant, k_{UISC}, can be computed in the framework of the Fermi Golden rule:[31,32]

$$k_{UISC} = \frac{2\pi}{\hbar}\rho_{FC}\,|\langle S_1|\hat{H}_{SO}|T_1\rangle|^2 \quad (1)$$

where $\langle S_1|\hat{H}_{SO}|T_1\rangle$ is the SOC matrix element between the S_1 and T_1 states, and ρ_{FC} denotes the Franck−Condon-weighted density of states. The ρ_{FC} terms were evaluated in the framework of Marcus−Levich−Jortner theory:[33,34]

DOI: 10.1021/jacs.6b12124
J. Am. Chem. Soc. 2017, 139, 4042−4051

$$\rho_{FC} = \frac{1}{\sqrt{4\pi\lambda_M k_B T}} \sum_{n=0}^{\infty} \exp(-S) \frac{S^n}{n!} \exp\left[-\frac{(\Delta E_{ST} + n\hbar\omega_{eff} + \lambda_M)^2}{4\lambda_M k_B T}\right] \quad (2)$$

where λ_M denotes the Marcus reorganization energy associated with the intermolecular and intramolecular low-frequency vibrations; k_B, the Boltzmann constant; T, temperature; $\hbar\omega_{eff}$, the effective energy of a mode representing the nonclassical high-frequency intramolecular vibrations $\left(\frac{\hbar\omega_{eff}}{k_B T} \gg 1\right)$; and S, the effective Huang–Rhys factor associated with this mode. Since the initial state for UISC is a triplet state (most often T_1 but sometimes T_2), all the calculations associated with the UISC rates are carried out at the relevant triplet-state geometries.

To set the stage for the remainder of our discussion, Figure 2 summarizes how a range of ΔE_{ST} values (between 0.0 and 0.4 eV) and

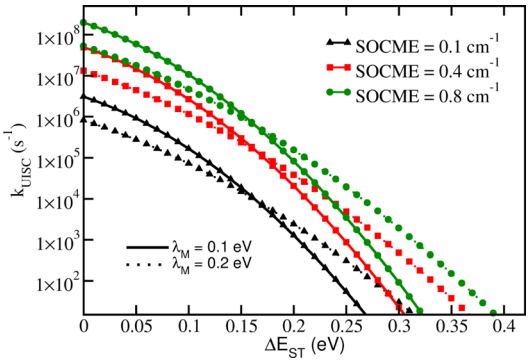

Figure 2. UISC rate constant as a function of ΔE_{ST} for different SOC matrix element (SOCME) and Marcus reorganization energy λ_M values (here, the effective Huang–Rhys factor S is ignored; see Tables S2 and S3).

of SOC matrix elements (between 0.1 and 0.8 cm^{-1}), according to eqs 1 and 2, influences the range of k_{UISC} rates for given λ_M values (*vide infra*). We note that since ΔE_{ST} is positive in general, ρ_{FC} is a decreasing function with respect to ΔE_{ST}. As expected, an enhanced SOC and a small ΔE_{ST} lead to fast UISC rates that can reach up to 10^8 s^{-1}. A smaller λ_M value is also found to be more favorable in the case of molecules with a sufficiently small ΔE_{ST} (≤0.16 eV in this case, see Figure 2).[35] In addition, for molecules with ΔE_{ST} larger than 0.4 eV, direct UISC from T_1 to S_1 states and hence TADF becomes negligible even with a SOC matrix element value as large as 0.8 cm^{-1}.[20,21,28−30,36] Importantly, a small reduction in ΔE_{ST} on the order of 50 meV can increase k_{UISC} by approximately 1 order of magnitude. Likewise, only a few tenths of cm^{-1} increase in the SOC matrix element value is sufficient to speed up UISC by over 1 order of magnitude. Thus, an in-depth understanding of the characteristics of the ΔE_{ST} and SOC terms is critical.

Molecular Electronic-Structure Calculations and ΔE_{ST}. All the molecules were optimized in their ground-state (S_0) at the DFT level of theory using the B3LYP hybrid functional[37−39] and 6-31G(d) basis set. The geometries in the excited states were optimized using the CAM-B3LYP functional; the S_1-state geometries were optimized at the TDDFT level, while the T_1 geometries were obtained via spin-unrestricted SCF calculations; the T_2-state geometries were also optimized at the TDDFT level where relevant. In order to account for matrix effects in the condensed phase and to allow a better comparison to available experimental data,[40] all calculations were conducted using the polarizable continuum model (PCM), taking the dielectric constant for toluene (ε = 2.37) as reference.[41]

As described in earlier works,[42,43] the excitation energies were calculated by employing the gap-tuned range-separated LC-ωPBE functional with the 6-31+G(d) basis set within the Tamm–Dancoff approximation (TDA); the optimal range-separation ω values were determined by minimizing J^2 as follows:[42−45]

$$J^2 = \sum_{i=0}^{1} [\varepsilon_H(N+i) + IP(N+i)]^2 \quad (3)$$

where IP and ε_H denote the ionization potential and HOMO energy of a given molecule, respectively, and N is the number of electrons in the molecule. We refer, hereafter, to the LC-ωPBE functional tuned ω value as LC-ω*PBE. The optimal ω values (Table S4 in Supporting Information) were taken from the previous report by Sun et al.[42] except for 4CzIPN-Me, which was calculated in this work; all other calculations including geometry optimizations were carried out again here. The adiabatic ΔE_{ST} values, defined as the difference between the energies of the potential minima for the S_1 and T_1 states, were then evaluated for all the molecules. Natural transition orbital (NTO) analyses were performed to examine the nature of the excited states.[46] The excited-state wave functions were further exploited to quantitatively evaluate their local-excitation (LE) and charge-transfer (CT) contributions, as discussed elsewhere (see also Supporting Information).[47] All the calculations described above were carried out with the Gaussian 09 code.[48]

Spin–OrbitCouplings. The SOC matrix elecment, $\langle S_1|\hat{H}_{SO}|T_1\rangle$, is calculated by considering that the three T_1 substates (m = 0, ±1) are degenerate, i.e., $\langle S_1|\hat{H}_{SO}|T_1\rangle = \sqrt{\sum_{m=0,\pm1} \langle S_1|\hat{H}_{SO}|T_1^m\rangle^2}$.[49] The spin–orbit coupling operator within the zeroth-order regular approximation (ZORA) is written as[50−52]

$$\hat{H}_{SO} = \frac{c^2}{(2c^2 - V)^2} \boldsymbol{\sigma} \cdot (\nabla V \times \mathbf{p}) \quad (4)$$

where $\boldsymbol{\sigma}$ represents the Pauli spin matrix vector; $\mathbf{p}$, the linear momentum operator; c, the speed of light; and V, the Kohn–Sham potential.

In the present calculations, SOC was treated as a perturbation based on the scalar relativistic (SR) orbitals after SCF and TDDFT calculations (pSOC-TDDFT);[52] TZP, the Slater-type all-electron basis set, was used for all the atoms.[53] In addition, matrix effects were also considered by using here the COSMO continuum solvation model.[54] Various exchange-correlation functionals, e.g., B3LYP, PBE0, BHandHLYP, and M06-2X, were tested[55] and PBE0 was chosen since the results were found to be most consistent with those obtained with the LC-ω*PBE functional that was employed for the electronic-structure calculations (see Tables S5 and S6). The SOC matrix elements for all the molecules were calculated using the ADF2014 package.[56]

Reorganization Energy. In the evaluation of k_{UISC}, the reorganization energy (λ) is one of the important factors that must be estimated. For a few representative molecules, the vibration relaxation energy of the S_1 state and the associated S factor were calculated using the DUSHIN program developed by Reimers.[57] The computed effective reorganization energies due to high-frequency, nonclassical intramolecular vibrations ($S\cdot\hbar\omega_{eff}$) are found to be ca. 0.01 eV for α-NPD and 0.19 eV for PXZ-TRZ, whereas the total intramolecular λ for those molecules are computed to be ca. 0.12 and 0.39 eV, respectively (see Supporting Information, Table S2). Thus, overall, the Marcus reorganization energy (λ_M in eq 2) due to low-frequency intramolecular vibrations and the surrounding medium-induced relaxations can be expected to fall in the range ~0.1–0.2 eV.[34,58] In addition, S factor is found to be safely ignored for the larger molecules. The theoretical background for λ and the effect of the neglect of S factor on the UISC rate are discussed in the Supporting Information in more detail.

3. RESULTS AND DISCUSSION

We begin first with the theoretical evaluation of the UISC rates for the organic emitters in this study and an assessment of their reliability. We then discuss in detail the factors affecting these

DOI: 10.1021/jacs.6b12124
J. Am. Chem. Soc. 2017, 139, 4042−4051

Table 1. Singlet−Triplet Energy Difference (ΔE_{ST}), Spin−Orbit Coupling Matrix Element (SOCME) Values, and Up-Conversion Intersystem Crossing Rates (k_{UISC}) at 300 K

	ΔE_{ST} (eV)			k_{UISC} (s^{-1})		
molecule	calcd	exptl[a]	SOCME (cm^{-1})	λ_M = 0.10 eV	λ_M = 0.20 eV	exptl
CBP	0.88	0.71	<0.01	<0.01	<0.01	
α-NPD	0.76	0.73	0.68	<0.01	<0.01	
2CzPN	0.25	0.31	0.74	2.1×10^3	1.2×10^4	5.4×10^3[e]
CC2TA	0.16 (0.13)[b]	0.20	0.30	1.1×10^5[d]	9.8×10^4[d]	1.6×10^5[f]
PIC-TRZ	0.11 (0.10)[b]	0.18	0.28[c]	1.1×10^6[d]	4.7×10^5[d]	
PXZ-TRZ	0.09 (0.01)[b]	0.06	1.54[c]	1.4×10^7[d]	3.9×10^6[d]	
ACRFLCN	0.02	0.24	0.46	4.3×10^7	1.2×10^7	
Spiro-CN	0.01 (−0.03)[b]	0.06	0.61[c]	4.8×10^7[d]	1.3×10^7[d]	
4CzIPN	0.01	0.10	0.27	1.83×10^7	4.92×10^6	2.7×10^6[g]
4CzIPN-Me	0.04	0.05	0.17	3.50×10^6	1.01×10^6	7.7×10^5[e]
4CzPN	0.00	0.15	0.61	1.14×10^8	3.07×10^7	
4CzTPN	0.06	0.09	0.81	4.43×10^7	1.41×10^7	
4CzTPN-Me	0.09	0.09	0.31	2.34×10^6	9.27×10^5	

[a]Experimental data taken from ref 40. [b]The calculated adiabatic energy differences between the S_1 and T_2 states are in parentheses; here, the negative value means that the T_2 state is higher in energy than the S_1 state. [c]These values correspond to T_2 to S_1 transitions. [d]The k_{UISC} values were calculated by taking into account the ISC not only directly from T_1 to S_1 but also from T_1 via T_2 to S_1; the relative population in the T_2 state with respect to that in the T_1 state was obtained by considering thermal equilibrium, i.e., the Boltzmann factor. [e]Ref 19. [f]Ref 18. [g]Ref 13.

Table 2. Molecules with Small Adiabatic Energy Difference between the T_1 and T_2 States (ΔE_{TT}): Spin−Orbit Coupling Matrix Element (SOCME) Values between the Respective Triplet States and the S_1 state, and Comparison of the Direct and Indirect Up-Conversion Intersystem Crossing Rates (k_{UISC}) at 300 K[a]

				k_{UISC} (s^{-1})			
		SOCME (cm^{-1})		λ_M = 0.10 eV		λ_M = 0.20 eV	
molecule	ΔE_{TT} (meV)	$T_1 \leftrightarrow S_1$	$T_2 \leftrightarrow S_1$	$T_1 \rightarrow S_1$	$T_1 \leftrightarrow T_2 \rightarrow S_1$	$T_1 \rightarrow S_1$	$T_1 \leftrightarrow T_2 \rightarrow S_1$
CC2TA	36	0.30	0.09	1.0×10^5	3.7×10^3	9.5×10^4	3.0×10^3
PIC-TRZ	−9[b]	0.11	0.28	1.4×10^5	9.2×10^5	6.5×10^4	4.0×10^5
PXZ-TRZ	−78[b]	0.26	1.54	1.7×10^6	1.2×10^7	6.5×10^5	3.3×10^6
ACRFLCN	5	0.46	0.01	4.3×10^7	1.9×10^4	1.2×10^7	5.0×10^3
Spiro-CN	−34[b]	0.01	0.61	3.0×10^4	4.8×10^7	8.2×10^3	1.3×10^7

[a]The indirect and direct UISCs represent the processes when passing or not via the T_2 state, respectively. [b]Negative values indicate that the charge-transfer triplet state is lower in energy than the local-excitation triplet state.

rates, with a focus on the ΔE_{ST} values and SOC matrix elements.

3.1. Up-Conversion Intersystem Crossing Rates. The k_{UISC} rates calculated at 300 K along with the ΔE_{ST} and SOC matrix element values are reported in Table 1. The computed rates are in reasonable agreement with the available experimental data, especially given that we arbitrarily set the λ_M value to either 0.1 or 0.2 eV and generally neglected UISC via higher electronic states. However, we considered UISC via the T_2 state for the cases of PIC-TRZ, PXZ-TRZ, and Spiro-CN, where the energy difference between the S_1 and T_2 states is small and the corresponding SOC matrix element is significant (*vide infra*). Importantly, the experimental and calculated k_{UISC} values are of the same order of magnitude. At 300 K, for instance, k_{UISC} for 2CzPN is experimentally measured as 5.4×10^3 s^{-1} while the calculated values is 2.1×10^3 s^{-1} with λ_M of 0.1 eV; the calculated k_{UISC} for CC2TA with the same λ_M is just 1.5 times smaller than the experimental value (1.1×10^5 s^{-1} vs 1.6×10^5 s^{-1}). In addition, the k_{UISC} values for 4CzIPN and 4CzIPN-Me are calculated to be some 1.8 and 1.3 times larger with a 0.2 eV λ_M than the experimental data (4.9×10^6 s^{-1} vs 2.7×10^6 s^{-1} for the former; 1.0×10^6 s^{-1} vs 7.7×10^5 s^{-1} for the latter).

The series of molecules we have considered in this study have ΔE_{ST} and SOC matrix element values in the ranges from 0.00 to 0.88 eV and from 0.00 to 1.54 cm^{-1}, respectively (we recall that the conversion factor eV and cm^{-1} is 1 eV = 8066 cm^{-1}). The calculated k_{UISC} values for the non-TADF molecules that have a large ΔE_{ST} are found to be negligible. Despite its relatively large SOC matrix element of 0.68 cm^{-1}, for instance, α-NTD is unlikely to undergo UISC directly from T_1 to S_1 at room temperature due to its high ΔE_{ST} value (0.76 eV).

We note that, among the molecules with moderate values of ΔE_{ST}, this parameter appears to play a more important role in determining k_{UISC} than SOC. For example, 2CzPN exhibits larger ΔE_{ST} and SOC matrix element values than CC2TA (0.25 eV vs 0.16 eV for ΔE_{ST} and 0.74 cm^{-1} vs 0.30 cm^{-1} for SOC matrix element, respectively). However, k_{UISC} has been measured to be about 30 times larger for CC2TA,[18,59] and our calculation also points to UISC being about 50 times faster with λ_M set at 0.1 eV. Expectedly, a stronger SOC enhances the UISC rate when the ΔE_{ST} values are similar; thus, the UISC rate of ACRFLCN is about twice higher than that of 4CzIPN (4.3×10^7 s^{-1} vs 1.8×10^7 s^{-1} with λ_M of 0.1 eV) while the ΔE_{ST} values are close (20 vs 10 meV). The 4CzIPN molecule exhibits a substantially smaller ΔE_{ST} than 4CzTPN (10 vs 60 meV), but the UISC for the former is twice as slow as for the latter (4.4×10^7 s^{-1} with λ_M of 0.1 eV), which is due to its three

DOI: 10.1021/jacs.6b12124
J. Am. Chem. Soc. 2017, 139, 4042−4051

times as small SOC matrix element value (0.27 cm^{-1} for 4CzIPN vs 0.81 cm^{-1} for 4CzTPN).

Interestingly, we find that UISC can occur on a fast time scale shorter than 100 ns at 300 K when the molecules are simultaneously on the lower side of the ΔE_{ST} range and higher side of the SOC range. This is the case for ACRFLCN, 4CzPN, and 4CzTPN. Their ΔE_{ST} values are calculated to be 20, 0, and 60 meV, respectively, and their SOC matrix element values, 0.46, 0.61, and 0.81 cm^{-1}.

It is also worth paying attention to Spiro-CN. This molecule has a negligible SOC matrix element between the S_1 and T_1 states (0.01 cm^{-1}; see Table 2); hence, the corresponding UISC is as slow as 3.0×10^4 s^{-1} with λ_M equal to 0.1 eV. However, the S_1 and T_2 states are close in energy with the T_2 state higher by 27 meV, and the energy difference between the T_1 and T_2 states is as small as 34 meV (Table 2). The computed SOC matrix element values and ISC rate (λ_M = 0.1 eV) between the T_2 and S_1 state are 0.61 cm^{-1} and 4.8×10^7 s^{-1}, respectively, with the latter value 3 orders of magnitude larger than for the process via T_1. Likewise, the T_2 states of PIC-TRZ and PXZ-TRZ are close in energy to the S_1 state (100 and 8 meV, respectively) and have LE character (*vide infra*); as a result, they have larger SOCs with the S_1 states than their T_1 counterparts (0.28 vs 0.11 cm^{-1} for PIC-TRZ and 1.54 vs 0.26 cm^{-1} for PXZ-TRZ, see Table 2), which leads to a 1 order of magnitude increase in k_{UISC}. Therefore, it can be expected that these molecules undergo UISC more significantly via their T_2 state.[28−30]

As an interesting counter-example, ACRFLCN also possesses T_1 and T_2 states with a very small energy difference of ca. 5 meV (Table 2). The SOC matrix element between the T_2 and S_1 states is, however, much smaller than that between the T_1 and S_1 states (0.01 vs 0.46 cm^{-1}, Table 2); such a small SOC results in a k_{UISC} rate from T_2 to S_1 on the order of 2.0×10^4 s^{-1} (λ_M = 0.1 eV), which is over 3 orders of magnitude smaller than that from T_1 to S_1 (4.3×10^7 s^{-1}). Therefore, UISC via the T_2 state can be ruled out for this molecule.

Our results underline that subtle changes in ΔE_{ST} and SOC matrix element values can have significant impacts on the UISC rates. We now turn to a discussion of the factors that determine the magnitudes of ΔE_{ST} and SOC.

3.2. Singlet−Triplet Energy Gap, ΔE_{ST}. In the restricted Hartree−Fock picture that has been pervasive in the discussion of TADF emitters, the exchange energy, *K*, between the hole (in the HOMO) and electron (in the LUMO) stabilizes the triplet excited state and destabilizes to the same extent the corresponding singlet excited state,[23,24] which leads to a ΔE_{ST} of 2*K*.[60] As stated earlier, however, the singlet and triplet excited states are often of a different nature; as a result, not only the exchange energy *K* but also the Coulomb integral, *J*, of the hole−electron pair and the relevant orbital energy difference *are different for the singlet and triplet excited states*;[23,24,61] furthermore, electron correlation effects can also play different roles in stabilizing the excitation energies of those two states.[24] Therefore, in reality, ΔE_{ST} *does not necessarily equate to 2K*. It is thus desirable to gain a better understanding of the factors governing ΔE_{ST}.

The calculated ΔE_{ST} values for the non-TADF emitters are the largest (0.88 and 0.76 eV for CBP and α-NPD, respectively, see Table 1) among the molecules studied here. This is related to the substantial LE nature in *both* T_1 and S_1 states. As reported in Table 3 and illustrated in Figure S2, CBP exhibits dominant LE characteristics (75.8%) for the lowest triplet excited state, leading to substantial *K* and thus significant ΔE_{ST}. Although the S_1 state exhibits a significant increase in CT character (46.9%) corresponding to a smaller *K*, the LE contribution to the S_1 state remains predominant. Likewise, see Figure S2, despite a more significant CT nature of the S_1 state (72.1%), α-NPD possesses a substantial LE character in the T_1 state (70.5%), indicating a larger overlap between the corresponding transition orbitals and thus a larger *K*. It is noteworthy that the comparatively smaller ΔE_{ST} value of α-NPD compared to that of CBP can be associated with its enhanced CT character in the S_1 state (72.1% vs 53.1%).

Table 3. Calculated Charge Transfer (CT) and Local Excitation (LE) Characters (in %) for the S_1 and T_1 States of the Molecules Considered in This Study

	S_1 state		T_1 state		
molecule	CT	LE	CT	LE	exptl[b]
CBP	53.1	46.9	24.2	75.8	LE
α-NPD	72.1	27.9	29.5	70.5	LE
2CzPN	91.7	8.3	50.6	49.4	LE
CC2TA	88.0	12.0	6.2	93.8	LE
PIC-TRZ	88.7	11.3	85.9 (1.7)[a]	14.1 (98.3)[a]	LE
PXZ-TRZ	91.4	8.6	79.1 (3.2)[a]	20.9 (96.8)[a]	CT
ACRFLCN	91.6	8.4	4.3 (90.9)[a]	95.7 (9.1)[a]	LE
Spiro-CN	97.9	2.1	96.2 (2.4)[a]	3.8 (97.6)[a]	LE
4CzIPN	89.1	10.9	77.6	22.4	LE
4CzIPN-Me	88.1	11.9	81.5	18.5	
4CzPN	91.0	9.0	70.3	29.7	LE
4CzTPN	87.6	12.4	73.0	27.0	CT
4CzTPN-Me	87.6	12.4	82.7	17.3	CT

[a]The LE and CT contributions to the T_2 state are in parentheses. [b]Ref 40.

The molecules composed of electron-donor (D) and electron-acceptor (A) units show, as expected, notably smaller ΔE_{ST} values. Taking the NTOs of 2CzPN and PIC-TRZ molecules as examples, see Figure S2, a clear CT character (∼90%) from D to A appears in the S_1 state, due to the spatial separation of the HOMO and LUMO, leading to a small *K* and small ΔE_{ST} value.[23,24,62] For the T_1 state of 2CzPN, however, a significant LE component appears (49.4%), while the LE character in the PIC-TRZ T_1 state remains limited (14.1%).[63] As a result, 2CzPN exhibits a substantially larger ΔE_{ST} (0.25 eV) than PIC-TRZ (0.11 eV). Turning to Spiro-CN, PXZ-TRZ, and 4CzPN, a significant CT character is observed in the T_1 states (from 70.3% to 96.2%) in addition to a predominant CT nature for their S_1 states (87.6−97.9%).[63] Consequently, ΔE_{ST} is calculated be less than 0.1 eV (0.00 eV for 4CzPN and 0.09 eV for PXZ-TRZ and 4CzTPN-Me).

In the case of ACRFLCN, ΔE_{ST} is small, ca. 20 meV, even though the T_1 state has a strong LE character and S_1 is predominantly CT in nature. The T_2 state of this molecule, however, is characterized as predominantly CT (90.9% of CT nature, see Figure 3 and Table 3) as in the S_1 state, which suggests a very small *K* for this triplet excited state and hence a very small energy difference between the S_1 and T_2 states. Given the 20 meV ΔE_{ST} between S_1 and T_1, the T_1 and T_2 states should be nearly isoenergetic; as mentioned earlier, the T_1−T_2 energy difference is calculated to be just ca. 5 meV (Table 2). Therefore, the small ΔE_{ST} of ACRFLCN should be ascribed to the energetic vicinity of the T_1 and T_2 states.

The question then arises as to when the triplet LE and CT states are close in energy? A useful starting point is to consider

DOI: 10.1021/jacs.6b12124
J. Am. Chem. Soc. 2017, 139, 4042−4051

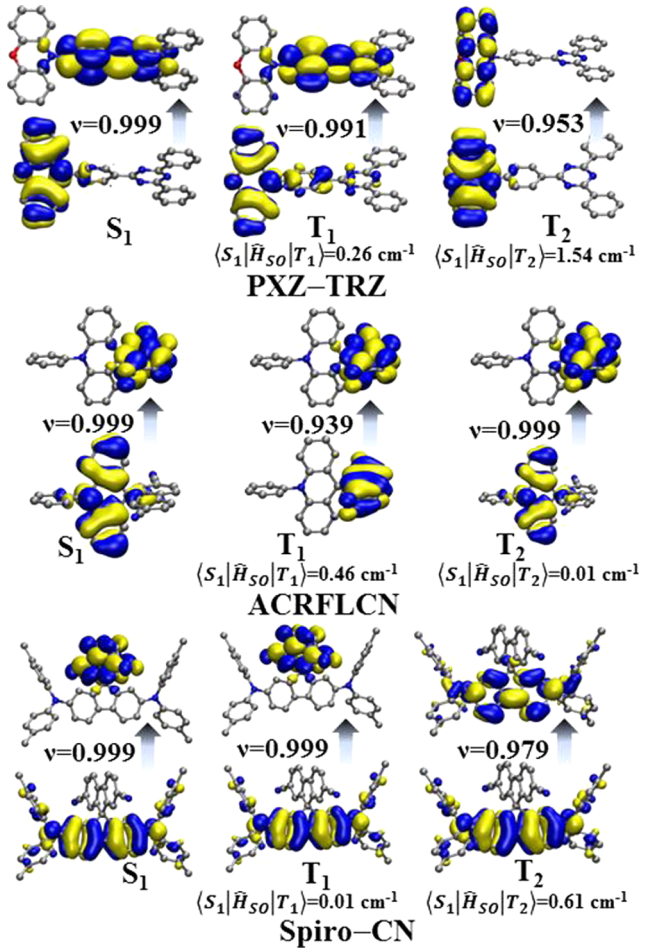

Figure 3. Natural Transition Orbital (NTO) pairs for the representative excited states of PXZ-TRZ, ACRFLCN and Spiro-CN along with spin–orbit coupling (SOC) matrix elements for the pair of relevant states. Hole and particle wave functions with the largest weight, ν, are placed below and above the arrows, respectively. Hydrogen atoms are omitted for the sake of clarity.

the HOMO–LUMO energy gap, $\Delta E_{\text{H-L}}$.[24,43,61] In the case of the CT triplet state, it is the $\Delta E_{\text{H-L}}$ calculated for the whole molecule that is relevant (with the HOMO localized on the donor subunit and the LUMO on the acceptor subunit: $\Delta E_{\text{H-L}}^{\text{CT}}$). For the LE triplet state, it is the $\Delta E_{\text{H-L}}$ calculated for the subunit (donor or acceptor: $\Delta E_{\text{H-L}}^{\text{LE}}$) on which the triplet exciton resides that is relevant. As we pointed out earlier, an LE character leads to a large K value and a strong stabilization of the LE triplet state energy. It is when $\Delta E_{\text{H-L}}^{\text{CT}}$ becomes small enough with respect to $\Delta E_{\text{H-L}}^{\text{LE}}$ that the CT triplet state energy can decrease sufficiently to compensate for its intrinsically smaller K.[24,61] Then, the CT triplet state can become energetically close to the LE triplet state, as in CC2TA and ACRFLCN, or even more stable than the triplet LE state, as in Spiro-CN and PXZ-TRZ. These four molecules have similar contributions from excitations within carbazole-type moieties in their LE triplet state (see Figures 3 and S2); hence, comparable exchange stabilization energies (as well as similar Coulombic and electron correlation contributions) can be expected for the LE triplet state. It is useful to consider the ratio of the calculated $\Delta E_{\text{H-L}}$ value for the whole molecule ($\Delta E_{\text{H-L}}^{\text{CT}}$) over the $\Delta E_{\text{H-L}}$ value for the carbazole subunit ($\Delta E_{\text{H-L}}^{\text{LE}}$):

$$\frac{\Delta E_{\text{H-L}}^{\text{CT}}}{\Delta E_{\text{H-L}}^{\text{LE}}} \tag{5}$$

In going from CC2TA to ACRFLCN and Spiro-CN, this ratio decreases from 0.87 to 0.80 and 0.78 (see Table S9); this trend follows the stabilization of the CT triplet energy vs the LE state energy, with ΔE_{TT} going from 36 to 5 meV and −34 meV (a negative value meaning here that the CT triplet state is more stable than the LE triplet state). In the case of PXZ-TRZ, this ratio is even smaller (0.71), which is consistent with the even larger energy difference between the CT (T_1) and LE (T_2) states for that molecule (−78 meV). In the case of 2CzPN and 4CzPN, the LE triplet states are more localized as they are found within a single phthalonitrile unit, which further increases the magnitude of K. 2CzPN and 4CzPN have the $\Delta E_{\text{H-L}}$ ratios in eq 5 equal to 0.76 and 0.71, respectively; this has the consequence that the T_1 state of the latter has a larger CT contribution (70.3% in 4CzPN vs 50.6% in 2CzPN).

To summarize the discussion thus far, a spatial separation of HOMO and LUMO significantly enhances the CT contribution to the S_1 state. On the other hand, for the T_1 state, given the increased stabilization of triplet excited states when larger K values are realized as is the case for local excitations, spatially separating the HOMO and LUMO does not necessarily lead to a dominant CT character in the T_1 state, which would be essential to ensure a small ΔE_{ST}. Rather, the T_1 state often possesses a significant LE character, which can result in a substantial ΔE_{ST} value. However, we have highlighted instances where either the CT T_2 state can become energetically close to the LE T_1 state or the T_1 state gains strong CT character.

3.3. Spin–Orbit Coupling. As shown in eq 1, the UISC rate is proportional to the square of the SOC matrix element. The calculated SOC matrix element values for the molecules in this study have been listed in Table 1. These SOC matrix elements remain, as expected, very small in comparison to those in molecules containing a heavy metal atom; they vary over a range that is approximately 2–3 orders of magnitude smaller than the value calculated for $Ir(ppy)_3$, ca. 114 cm^{-1}.[64] However, as we underlined above, it is important to bear in mind that a change in these values over a few tenths of a cm^{-1} can significantly modulate the UISC rate.

A further detailed discussion of the $\hat{H}_{\text{SO}}$ operator can aid in the interpretation of our results. Using the central-field approximation where the potential energy for an electron, V, is a function of $\mathbf{r}$ between electron i and nucleus μ, eq 4 further reads as

$$\hat{H}_{\text{SO}} = \sum_{\mu}\sum_{i} \frac{2c^2}{(2c^2 - V_{\mu i})^2}\frac{1}{r_{\mu i}}\frac{\partial V_{\mu i}}{\partial r_{\mu i}}\left[\frac{1}{2}(\hat{l}_{\mu i+}\cdot\hat{s}_{i-} + \hat{l}_{\mu i-}\cdot\hat{s}_{i+}) + \hat{l}_{\mu iz}\cdot\hat{s}_{iz}\right] \tag{6}$$

where $\hat{l}_{\pm}[\hat{s}_{\pm}]$ stands for raising (+) or lowering (−) operator for the orbital [spin] angular momentum of a given electron; $\hat{l}_z[\hat{s}_z]$, denotes the z component of the orbital angular momentum operator, $\hat{l}$ [the spin momentum operator, $\hat{s}$] of the electron. This equation implies that, upon flipping the spin angular momentum of an electron up ($\hat{s}_+$), the orbital angular momentum of the electron must be lowered ($\hat{l}_-$), and *vice versa*, so as to conserve the total angular momentum. Since organic molecules in this study do not contain heavy atoms with d atomic orbitals, only the angular momentum of electrons

DOI: 10.1021/jacs.6b12124
J. Am. Chem. Soc. 2017, 139, 4042–4051

in p atomic orbitals are affected by $\hat{H}_{SO}$. When a given p_z (p_0) atomic orbital participating in a π-bond is involved, for example, upon flipping the spin up, the $\hat{l}_-$ operators convert the p_0 orbital of the electron into p_{-1}. Since p_{-1} is a linear combination of p_x and p_y orbitals, such an atomic orbital no longer participates in the π-bond; the opposite situation can also be readily expected. Consequently, when the spin of an electron is flipped over, $\hat{H}_{SO}$ either suppresses or reinforces π-conjugation, leading to a different extent of π-conjugation. Therefore, the SOC matrix element value for ISC can be qualitatively estimated by evaluating the changes in π-conjugation of either hole or electron wave functions, between the singlet and triplet excited states. This is in line with the *El-Sayed rule*, i.e., the rate of ISC becomes faster when the ISC process involves a change in orbital type.[65,66] It should be borne in mind, however, that if the π-conjugation changes in both hole and electron wave functions, such changes correspond to spin-flips of both hole and electron; then, the system remains in the same spin multiplicity and the SOC for ISC is suppressed.[64,67]

In the case of ACRFLCN, the S_1 state has a predominant CT nature (91.6%), while the T_1 state is predominantly a LE state (95.7%), see Figure 3 and Table 3. This difference in the nature of the excited states gives rise to a significant SOC matrix element value of 0.46 cm^{-1}. On the other hand, in Spiro-CN, the S_1 and T_1 states both have a significant CT character (97.9% and 96.2%, respectively, see Table 3), leading to a negligible SOC matrix element value of 0.01 cm^{-1}; as detailed above, however, the T_2 state is characterized as a LE state within the donor subunit (97.6%); hence, the SOC matrix element value between the S_1 and T_2 states is as large as 0.61 cm^{-1}. PXZ-TRZ exhibits an even stronger SOC matrix element value (1.54 cm^{-1}) between the S_1 and T_2 states,[68] which is again understood by their marked difference in nature (CT vs LE state, respectively, see Figure 3).[14,16,22,29] For PIC-TRZ, despite a distinct difference in nature (CT vs LE), the SOC matrix element values between the S_1 and T_2 states is smaller (0.28 cm^{-1}) because of π-conjugation changes in both hole and electron wave functions (Figure S2).

In the cases of 4CzPN and 4CzTPN, the calculated SOC matrix element values are relatively high: 0.61 and 0.81 cm^{-1}, respectively. However, those of 4CzIPN and 4CzIPN-Me remain moderate: 0.27 and 0.17 cm^{-1}, respectively. CT contributions in the S_1 state of all 4CzPN analogues are as high as 87.6−91.0% and those for the T_1 states are also in the range between 70.3% and 82.7%. Therefore, such variations in the SOC matrix element values are puzzling. A closer observation of NTO pairs, however, reveals an important difference among this series of molecules. Since, the SOC matrix elements are calculated at the T_1-state geometries, it is more appropriate to compare the natures of the S_1 and T_1 states at those geometries, see Figure 4. We first note that all of these molecules have similar electron wave functions in both S_1 and T_1 states. The differences are to be found in the hole wave functions. In the molecules with higher SOC matrix elements (4CzPN and 4CzTPN), it appears that *different* carbazole subunits are involved in the electronic transitions to the S_1 and T_1 states. For instance, in 4CzPN, it is the carbazole units in *ortho* with respect to the cyano substituents that are mainly involved in the hole wave function of the S_1 state, while the neighboring *meta*-carbazole units are a major component of the T_1 state; this points to different distributions of π-conjugation in the hole wave functions for the T_1 and S_1 states, as we have observed in the cases of LE triplet vs CT singlet states. In the

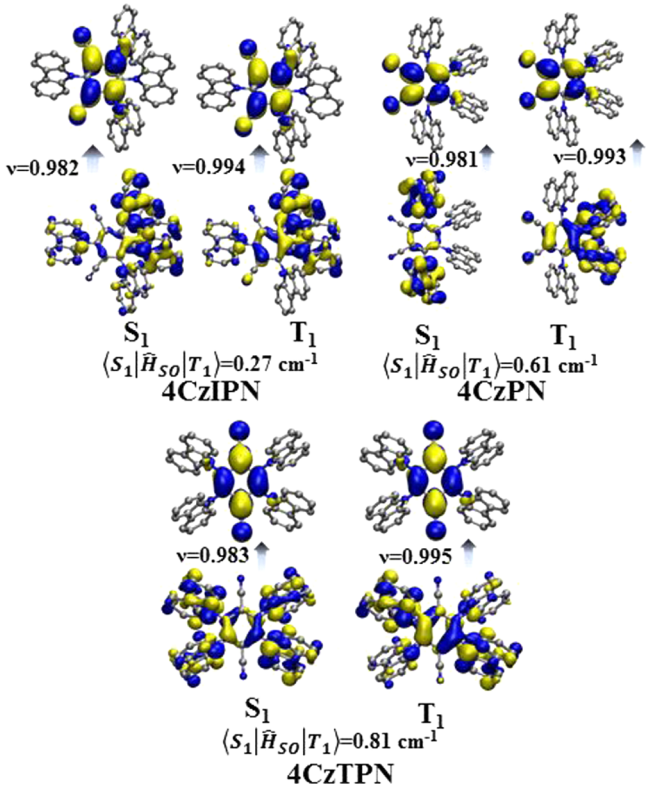

Figure 4. Natural Transition Orbitals (NTOs) for the S_1 and T_1 states of 4CzIPN, 4CzPN, and 4CzTPN at their T_1-state geometries. Hole and particle wave functions with the largest weight, ν, are placed below and above the arrows, respectively. Spin−orbit coupling (SOC) matrix elements are also provided. Hydrogen atoms are omitted for the sake clarity.

case of 4CzTPN, all four carbazole units make nearly equal contributions to the hole wave function of the S_1 state, while only two of them contribute significantly to the T_1 state (a feature again in line with the tendency of triplet wave functions to be more contracted in order to maximize K), which points to different distributions of π-conjugation. Recalling that an efficient ISC requires a change in π-conjugation of either hole or electron wave function (see section 2), such differences in the π-conjugation of the hole wave functions between the S_1 and T_1 states is consistent with the substantial SOC matrix element values for 4CzPN and 4CzTPN. On the other hand, in the 4CzIPN derivatives, the differences in hole wave functions for the S_1 and T_1 states are not as significant, which leads to relatively smaller SOC matrix element values. These results highlight, as expected from eq 6, the importance of variations in the π-conjugation of either hole or electron wave functions in the course of the ISC process.

3.4. Design Rules for Efficient Up-Conversion ISC. In order to increase the UISC rates, the case is clear that ΔE_{ST} should be minimized and spin−orbit coupling should be maximized. Since the S_1 state of a donor−acceptor molecule usually corresponds to the transition from HOMO (on the donor subunit) to LUMO (on the acceptor subunit) and displays a dominant charge-transfer character, it is the triplet excited state with a local-excitation nature that naturally leads to a strong SOC with the S_1 state. As a result, this LE triplet state should be energetically close to the S_1 state.[22] Given that the S_1 state and its corresponding CT triplet state are necessarily close in energy, this requirement in turn translates into an energetic

DOI: 10.1021/jacs.6b12124
J. Am. Chem. Soc. 2017, 139, 4042−4051

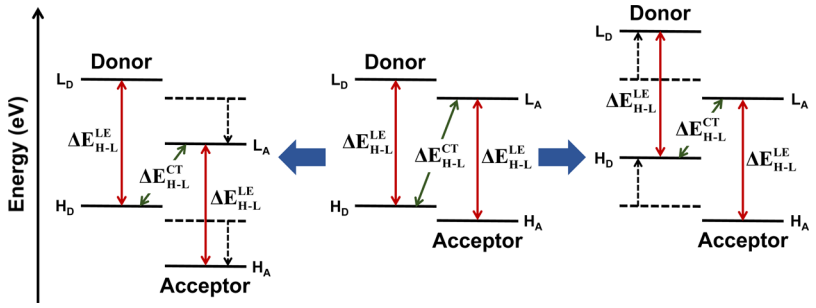

Figure 5. Schematic illustration of the modulation of the HOMO−LUMO energy gap for the CT triplet state of a donor−acceptor molecule (ΔE^{CT}_{H-L}) with respect to the HOMO−LUMO gap for the LE triplet state (ΔE^{LE}_{H-L}). H_D [H_A] and L_D [L_A] denote the HOMO and LUMO of the donor [acceptor] unit, respectively. Note that the HOMO and LUMO of the whole donor−acceptor molecule correspond to H_D and L_A, respectively.

proximity between the LE and CT triplet states. As was amply discussed earlier, LE triplet states are generally more stable than their CT counterparts. Given that the energy of the CT state is far more sensitive to ΔE_{H-L} than that of the LE state,[61] it is much easier to reduce ΔE_{ST} by manipulating the former, i.e., by reducing the ΔE_{H-L} of the donor−acceptor molecule for a given combination of donor and acceptor subunits, one of which determines the LE triplet state energy. Ways to fulfill this goal are to stabilize to the same extent the HOMO and LUMO energy levels of the acceptor subunits, or to destabilize those of the donor subunits, as illustrated in Figure 5.

In this context, it is useful to recall that carbazole has long been exploited as a typical donor subunit. We have demonstrated earlier that carbazole can inductively pull some electron density from an adjacent acceptor and such an effect is additive when increasing the number of carbazole units;[25−27,61] hence, additional carbazole(s) further stabilize to a similar extent the HOMO and LUMO of the neighboring acceptor subunit, with little modification of the (local) ΔE_{H-L} value of carbazole subunit itself. Furthermore, when several of the same donor or acceptor units are employed, some of them likely find themselves in chemically different environments; combined with a small ΔE_{ST} (induced by the use of several, for example, carbazole units), this can lead to different natures for the S_1 vs T_1 states, and hence enhanced UISC, even when both the S_1 and T_1 states have a dominant CT character. As discussed earlier, the four carbazole groups in 4CzPN are in two distinctive environments, i.e., *ortho*- vs *meta*-positions with respect to the closest cyano substituent; the carbazole units at the latter positions are more prone to secure a larger LE character; hence, the S_1 and T_1 states have different hole wave functions. Likewise, the carbazole groups of 4CzTPN are in two inequivalent positions, as they connect to the core terephthalonitrile unit at either large or small amplitudes of the hole wave functions, see Figure 4. As a result, only two of the carbazole units are involved in more contracted hole wave functions for the T_1 state because of the larger K stabilization the triplet can then achieve.

4. SYNOPSIS

We have evaluated the up-conversion (also known as "reverse") intersystem crossing rates, k_{UISC}, for a series of organic emitters relevant for thermally activated delayed fluorescence (TADF). The good agreement with available experimental data has allowed us to theoretically explore, on reliable grounds, the factors influencing k_{UISC}, i.e., the energy difference between the lowest singlet and triplet excited states, ΔE_{ST}, and the strength of spin−orbit coupling, SOC. The UISC rates are faster, the smaller the ΔE_{ST} values and the larger the SOC. In spite of significantly weaker SOC in comparison to heavy-atom containing phosphors (by 2−3 orders of magnitude), we find that UISC in TADF organic materials can occur on a time scale shorter than 100 ns at 300 K.

With regard to lessening ΔE_{ST}, we conclude that spatially separating the HOMO and LUMO wave functions in donor−acceptor-type organic emitters is not a sufficient criterion. Indeed, the lowest triplet excited state tends to have a local-excitation character, as this maximizes the exchange energy and thus minimizes its energy. What is required is to stabilize the lowest triplet state with a charge-transfer character or to enhance the CT contribution to the T_1 state. This can be achieved by decreasing significantly the HOMO−LUMO energy gap in the donor−acceptor molecule with respect to the HOMO−LUMO gap for the subunit (donor or acceptor) on which the triplet exciton tends to localize.

The spin−orbit coupling can be strengthened by making different the natures of the relevant excited singlet and triplet states, which is consistent with the El-Sayed rule. Our results underline that, in up-converting from the lowest triplet to the lowest singlet excited state, a marked change in the π-conjugation pattern of either the hole or electron wave function is critical. To enhance the UISC rate then requires: either to up-convert from a LE triplet to a CT singlet state while succeeding in having these two states very close in energy, as described above; or to have a significant CT contribution to the T_1 state while achieving significant differences in the π-conjugation patterns of the hole or electron wave functions. Regarding the latter aspect, it is has been found useful to rely on multiple, identical donor or acceptor subunits. The design rules to which our work points, have been detailed in section 3.4.

Finally, we recall that the photoluminescence quantum yield (PLQY) also plays a critical role in the TADF process. For instance, the PLQY of 4CzIPN was reported to be 93.8%, while those of 4CzPN and 4CzTPN were measured to be 74.4 and 71.6%, respectively.[17] As a result, 4CzIPN has demonstrated to be one of the most efficient TADF materials to date, despite the fact that our calculations point to a one-order-of-magnitude smaller k_{UISC} than in 4CzPN. Thus, further systematic studies including the PLQYs of TADF materials are also required; these would have to evaluate, in the condensed phase, not only the prompt fluorescence efficiency itself but the nonradiative decay rates from the T_1 state to the ground state as well, a challenging theoretical/computational proposition.

DOI: 10.1021/jacs.6b12124
J. Am. Chem. Soc. 2017, 139, 4042−4051

■ ASSOCIATED CONTENT

Supporting Information

The Supporting Information is available free of charge on the ACS Publications website at DOI: 10.1021/jacs.6b12124.

Detailed description of the theoretical backgrounds for the gap-tuned, range-separated exchange-correlation functional, a quantitative assessment of the LE and CT contributions in the excited states, and orbital overlaps between hole and electron wave functions; calculated and experimental values of vertical excitation energies for the S_1 state, $E_{VA}(S_1)$, and the vertical singlet−triplet energy difference, $\Delta E_{ST\text{-}v}$, at the ground-state geometries; calculated values of SOC matrix elements at T_1 geometries; calculated intramolecular reorganization energies for organic emitters in this study and calculated effective reorganization energy from high-frequency vibrational modes for a few chosen molecules; comparison of the calculated UISC rates with and without consideration of the Huang−Rhys factor; calculated overlap between hole and electron wave functions for the S_1 and T_1 states; calculated HOMO−LUMO energy gaps for representative emitters and their subunits associated with the lowest LE triplet state; calculated vertical transition energies at the ground-state geometries using various exchange-correlation functionals; natural transition orbital pairs for the S_1 and T_1states of all molecules in this study (PDF)

■ AUTHOR INFORMATION

Corresponding Authors

*dongwook-kim@kyonggi.ac.kr

*jean-luc.bredas@kaust.edu.sa.

ORCID

Pralok K. Samanta: 0000-0002-1926-7720

Dongwook Kim: 0000-0003-2096-3720

Jean-Luc Brédas: 0000-0001-7278-4471

Notes

The authors declare no competing financial interest.

■ ACKNOWLEDGMENTS

This work was supported by King Abdullah University of Science and Technology (KAUST). We acknowledge the IT Research Computing Team and Supercomputing Laboratory at KAUST for providing computational and storage resources as well as precious assistance. The portion of this work carried out at Kyonggi University was supported by the Basic Science Research Program through the National Research Foundation of Korea (NRF) funded by the Ministry of Education, Science, and Technology (2015R1D1A1A01061487). D.K. also thanks Dr. Johannes Gierschner (Madrid Institute for Advanced Studies) for stimulating discussions regarding TADF.

■ REFERENCES

(1) Baldo, M. A.; Thompson, M. E.; Forrest, S. R. *Nature* **2000**, *403*, 750−753.

(2) Sun, Y. R.; Giebink, N. C.; Kanno, H.; Ma, B. W.; Thompson, M. E.; Forrest, S. R. *Nature* **2006**, *440*, 908−912.

(3) Evans, R. C.; Douglas, P.; Winscom, C. J. *Coord. Chem. Rev.* **2006**, *250*, 2093−2126.

(4) Lamansky, S.; Djurovich, P.; Murphy, D.; Abdel-Razzaq, F.; Lee, H. E.; Adachi, C.; Burrows, P. E.; Forrest, S. R.; Thompson, M. E. *J. Am. Chem. Soc.* **2001**, *123*, 4304−4312.

(5) Kamtekar, K. T.; Monkman, A. P.; Bryce, M. R. *Adv. Mater.* **2010**, *22*, 572−582.

(6) Tang, C. W.; Vanslyke, S. A. *Appl. Phys. Lett.* **1987**, *51*, 913−915.

(7) Reineke, S.; Lindner, F.; Schwartz, G.; Seidler, N.; Walzer, K.; Lüssem, B.; Leo, K. *Nature* **2009**, *459*, 234−238.

(8) Chi, Y.; Chou, P.-T. *Chem. Soc. Rev.* **2010**, *39*, 638−655.

(9) Kim, S.-Y.; Jeong, W.-I.; Mayr, C.; Park, Y.-S.; Kim, K.-H.; Lee, J.-H.; Moon, C.-K.; Brütting, W.; Kim, J.-J. *Adv. Funct. Mater.* **2013**, *23*, 3896−3900.

(10) Birks, J. B. *Ber. Bunsenges. Phys. Chem.* **1970**, *74*, 1294−1295.

(11) Obolda, A.; Peng, Q.; He, C.; Zhang, T.; Ren, J.; Ma, H.; Shuai, Z.; Li, F. *Adv. Mater.* **2016**, *28*, 4740−4746.

(12) Kondakov, D. Y.; Pawlik, T. D.; Hatwar, T. K.; Spindler, J. P. *J. Appl. Phys.* **2009**, *106*, 124510.

(13) Ishimatsu, R.; Matsunami, S.; Shizu, K.; Adachi, C.; Nakano, K.; Imato, T. *J. Phys. Chem. A* **2013**, *117*, 5607−5612.

(14) Santos, P. L.; Ward, J. S.; Data, P.; Batsanov, A. S.; Bryce, M. R.; Dias, F. B.; Monkman, A. P. *J. Mater. Chem. C* **2016**, *4*, 3815−3824.

(15) By definition, intersystem crossing (ISC) is a nonradiative interconversion process between two electronic states with different multiplicities. Thus, radiationless transitions between a singlet state and a triplet state (or between a doublet and a quartet state) correspond to ISC. Since triplet excited states are in general lower in energy than their singlet counterparts, we refer the ISC from the T_1 state to the S_1 state to up-conversion ISC (UISC), and that in the opposite direction to down-conversion ISC (DISC). We note that UISC is also often referred to in the literature as reverse ISC (RISC).

(16) Dias, F. B.; Santos, J.; Graves, D. R.; Data, P.; Nobuyasu, R. S.; Fox, M. A.; Batsanov, A. S.; Palmeira, T.; Berberan-Santos, M. N.; Bryce, M. R.; Monkman, A. P. *Adv. Sci.* **2016**, *3*, 1600080.

(17) Uoyama, H.; Goushi, K.; Shizu, K.; Nomura, H.; Adachi, C. *Nature* **2012**, *492*, 234−238.

(18) Lee, S. Y.; Yasuda, T.; Nomura, H.; Adachi, C. *Appl. Phys. Lett.* **2012**, *101*, 093306.

(19) Furukawa, T.; Nakanotani, H.; Inoue, M.; Adachi, C. *Sci. Rep.* **2015**, *5*, 8429−8429.

(20) Ogiwara, T.; Wakikawa, Y.; Ikoma, T. *J. Phys. Chem. A* **2015**, *119*, 3415−3418.

(21) Hontz, E.; Chang, W.; Congreve, D. N.; Bulović, V.; Baldo, M. A.; Van Voorhis, T. *J. Phys. Chem. C* **2015**, *119*, 25591−25597.

(22) Nobuyasu, R. S.; Ren, Z.; Griffiths, G. C.; Batsanov, A. S.; Data, P.; Yan, S.; Monkman, A. P.; Bryce, M. R.; Dias, F. B. *Adv. Opt. Mater.* **2016**, *4*, 597−607.

(23) Kim, D. *J. Phys. Chem. C* **2015**, *119*, 12690−12697.

(24) Kim, D. *Int. J. Quantum Chem.* **2016**, *116*, 651−655.

(25) Salman, S.; Kim, D.; Coropceanu, V.; Brédas, J. L. *Chem. Mater.* **2011**, *23*, 5223−5230.

(26) Kim, D.; Zhu, L.; Brédas, J. L. *Chem. Mater.* **2012**, *24*, 2604−2610.

(27) Kim, D.; Coropceanu, V.; Brédas, J. L. *J. Am. Chem. Soc.* **2011**, *133*, 17895−17900.

(28) Chen, X. K.; Zhang, S. F.; Fan, J. X.; Ren, A. M. *J. Phys. Chem. C* **2015**, *119*, 9728−9733.

(29) Gibson, J.; Monkman, A. P.; Penfold, T. J. *ChemPhysChem* **2016**, *17*, 2956−2961.

(30) Marian, C. M. *J. Phys. Chem. C* **2016**, *120*, 3715−3721.

(31) Lawetz, V.; Siebrand, W.; Orlandi, G. *J. Chem. Phys.* **1972**, *56*, 4058−4072.

(32) Robinson, G. W.; Frosch, R. P. *J. Chem. Phys.* **1963**, *38*, 1187−1203.

(33) Brédas, J. L.; Beljonne, D.; Coropceanu, V.; Cornil, J. *Chem. Rev.* **2004**, *104*, 4971−5003.

(34) Schmidt, K.; Brovelli, S.; Coropceanu, V.; Beljonne, D.; Cornil, J.; Bazzini, C.; Caronna, T.; Tubino, R.; Meinardi, F.; Shuai, Z.; Brédas, J. L. *J. Phys. Chem. A* **2007**, *111*, 10490−10499.

(35) When the same SOC matrix element value is assumed and the Huang−Rhys factor is ignored, the smaller λ_M value is favored when

$$\Delta E_{ST} \leq \sqrt{\lambda'_M \lambda''_M + \frac{2\lambda'_M \lambda''_M k_B T}{(\lambda''_M - \lambda'_M)} \ln \frac{\lambda''_M}{\lambda'_M}}$$

; at 300 K, when comparing between λ'_M and λ''_M of 0.1 and 0.2 eV, respectively, k_{UISC} is higher when $\Delta E_{ST} \leq 0.16$ eV.

(36) We note recent reports (refs 28−30) that stressed the role of the vibronic coupling between the T_1 and higher triplet excited states. In such a case, TADF might be observed. In addition, hyperfine interactions between nucleus and electron spins can contribute to the ISC (refs 20, 21); however, such an effect is expected to be small for TADF molecules (ref 29) and hence is not considered in this study.

(37) Becke, A. D. *J. Chem. Phys.* **1993**, *98*, 5648−5652.

(38) Lee, C. T.; Yang, W. T.; Parr, R. G. *Phys. Rev. B: Condens. Matter Mater. Phys.* **1988**, *37*, 785−789.

(39) Miehlich, B.; Savin, A.; Stoll, H.; Preuss, H. *Chem. Phys. Lett.* **1989**, *157*, 200−206.

(40) Huang, S.; Zhang, Q.; Shiota, Y.; Nakagawa, T.; Kuwabara, K.; Yoshizawa, K.; Adachi, C. *J. Chem. Theory Comput.* **2013**, *9*, 3872−3877.

(41) Scalmani, G.; Frisch, M. J. *J. Chem. Phys.* **2010**, *132*, 144110.

(42) Sun, H.; Zhong, C.; Brédas, J. L. *J. Chem. Theory Comput.* **2015**, *11*, 3851−3858.

(43) Penfold, T. J. *J. Phys. Chem. C* **2015**, *119*, 13535−13544.

(44) Kronik, L.; Stein, T.; Refaely-Abramson, S.; Baer, R. *J. Chem. Theory Comput.* **2012**, *8*, 1515−1531.

(45) Bokareva, O. S.; Grell, G.; Bokarev, S. I.; Kuehn, O. *J. Chem. Theory Comput.* **2015**, *11*, 1700−1709.

(46) Martin, R. L. *J. Chem. Phys.* **2003**, *118*, 4775−4777.

(47) Kim, D. *Bull. Korean Chem. Soc.* **2015**, *36*, 2284−2289.

(48) Frisch, M. J.; Trucks, G. W.; Schlegel, H. B.; Scuseria, G. E.; Robb, M. A.; Cheeseman, J. R.; Scalmani, G.; Barone, V.; Mennucci, B.; Petersson, G. A.; Nakatsuji, H.; Caricato, M.; Li, X.; Hratchian, H. P.; Izmaylov, A. F.; Bloino, J.; Zheng, G.; Sonnenberg, J. L.; Hada, M.; Ehara, M.; Toyota, K.; Fukuda, R.; Hasegawa, J.; Ishida, M.; Nakajima, T.; Honda, Y.; Kitao, O.; Nakai, H.; Vreven, T.; Montgomery, J. A., Jr.; Peralta, J. E.; Ogliaro, F.; Bearpark, M. J.; Heyd, J.; Brothers, E. N.; Kudin, K. N.; Staroverov, V. N.; Kobayashi, R.; Normand, J.; Raghavachari, K.; Rendell, A. P.; Burant, J. C.; Iyengar, S. S.; Tomasi, J.; Cossi, M.; Rega, N.; Millam, N. J.; Klene, M.; Knox, J. E.; Cross, J. B.; Bakken, V.; Adamo, C.; Jaramillo, J.; Gomperts, R.; Stratmann, R. E.; Yazyev, O.; Austin, A. J.; Cammi, R.; Pomelli, C.; Ochterski, J. W.; Martin, R. L.; Morokuma, K.; Zakrzewski, V. G.; Voth, G. A.; Salvador, P.; Dannenberg, J. J.; Dapprich, S.; Daniels, A. D.; Farkas, Ö.; Foresman, J. B.; Ortiz, J. V.; Cioslowski, J.; Fox, D. J. *Gaussian 09*, Revision D.01; Gaussian, Inc.: Wallingford, CT, 2009.

(49) Hu, D.; Yao, H.; Yang, B.; Ma, Y. *Philos. Trans. R. Soc., A* **2015**, *373*, 20140318.

(50) van Lenthe, E.; Snijders, J. G.; Baerends, E. J. *J. Chem. Phys.* **1996**, *105*, 6505−6516.

(51) van Lenthe, E.; van Leeuwen, R.; Baerends, E. J.; Snijders, J. G. *Int. J. Quantum Chem.* **1996**, *57*, 281−293.

(52) Wang, F.; Ziegler, T. *J. Chem. Phys.* **2005**, *123*, 154102.

(53) van Lenthe, E.; Baerends, E. J. *J. Comput. Chem.* **2003**, *24*, 1142−1156.

(54) Pye, C. C.; Ziegler, T. *Theor. Chem. Acc.* **1999**, *101*, 396−408.

(55) In the absence of experimental SOC values, the tests were conducted based on the vertical singlet excitation energies and vertical singlet−triplet energy differences in comparison to the results obtained with the LC-ω*PBE functional, which is found to be reliable in the calculation of TADF molecules (ref 42). In addition, the natures of the several lowest lying excited states are the same for both functionals (see Table S7); we note, however, that the ordering of the T_1 and T_2 states of ACR-FLCN is different, which was taken into account in the computation of the SOC and the UISC rate.

(56) Baerends, E. J.; Ziegler, T.; Atkins, A. J.; Autschbach, J.; Bashford, D.; Bérces, A.; Bickelhaupt, F. M.; Bo, C.; Boerrigter, P. M.; Carstensen, N. O.; Cavallo, L.; Chong, D. P.; Chulhai, D. V.; Deng, L.; Dickson, R. M.; Ellis, D. E.; van Faassen, M.; Fan, L.; Fischer, T. H.; Fonseca Guerra, C.; Franchini, M.; Ghysels, A.; Giammona, A.; van Gisbergen, S. J. A.; Götz, A. W.; Gritsenko, O. V.; Groeneveld, J. A.; Groot, L.; Grüning, M.; Gusarov, S.; Harris, F. E.; van den Hoek, P.; Jacob, C. R.; Jacobsen, H.; Jensen, L.; Kadantsev, E. S.; Kaminski, J. W.; van Kessel, G.; Kootstra, F.; Kovalenko, A.; van Krykunov, M. V.; Lenthe, E., Michalak, D. A. M.; Mitoraj, A. M.; Morton, S. M.; Neugebauer, J.; Nicu, V. P.; Noodleman, L., Patchkovskii, V. P. O.; Pavanello, S. M.; Philipsen, P. H. T.; Post, D.; Pye, C. C.; Ravenek, W.; Ros, J. I. R.; Schipper, P. R. T.; Schreckenbach, G.; Seldenthuis, J. S.; Seth, M.; Snijders, J. G., Swart, M. S.; Swerhone, M. D.; te Velde, G.; Vernooijs, P.; Versluis, L.; Visscher, L.; Visser, O.; Wang, F.; Wesolowski, T. A.; van Wezenbeek, E. M.; Wiesenekker, G.; Wolff, S. K.; Woo, T. K.; Yakovle, A. L. *ADF 2014*; SCM, Theoretical Chemistry, Vrije Universiteit: Amsterdam, The Netherlands; http://www.scm.com.

(57) Reimers, J. R. *J. Chem. Phys.* **2001**, *115*, 9103−9109.

(58) Beljonne, D.; Shuai, Z.; Pourtois, G.; Brédas, J. L. *J. Phys. Chem. A* **2001**, *105*, 3899−3907.

(59) Masui, K.; Nakanotani, H.; Adachi, C. *Org. Electron.* **2013**, *14*, 2721−2726.

(60) Köhler, A.; Bässler, H. *Mater. Sci. Eng., R* **2009**, *66*, 71−109.

(61) Lee, K.; Kim, D. *J. Phys. Chem. C* **2016**, *120*, 28330−28336.

(62) Kim, D. *Bull. Korean Chem. Soc.* **2014**, *35*, 2738−2742.

(63) In the cases of PIC-TRZ and Spiro-CN, the natures of the T_1 states in this study are different from those in the literature (Table 3); however, the T_2 states of such molecules are very close to their T_1 states in energy (9 and 34 meV, respectively), which helps explain the ordering changes in these molecules. In the cases of 4CzPN analogues, we note that our results tend to overestimate the CT contributions with respect to the results in the literature (refs 40 and 61), pointing to the effect of the nature of the chosen DFT functionals.

(64) Kleinschmidt, M.; van Wüllen, C.; Marian, C. M. *J. Chem. Phys.* **2015**, *142*, 094301.

(65) El-Sayed, M. *J. Chem. Phys.* **1963**, *38*, 2834−2838.

(66) Marian, C. M. *WIREs Comput. Mol. Sci.* **2012**, *2*, 187−203.

(67) Li, E. Y. T.; Jiang, T. Y.; Chi, Y.; Chou, P. T. *Phys. Chem. Chem. Phys.* **2014**, *16*, 26184−26192.

(68) In the case of PXZ-TRZ, supplementary calculations reveal that the SOC value between the singlet CT and triplet LE states significantly decreases (ca. 0.06 cm^{-1}) when its N and O atoms are replaced with CH and CH_2 groups, respectively, demonstrating the effect of the presence of such atoms with larger nucleus charges than C. Furthermore, the electron wave functions for the singlet CT and triplet LE states appear to be more confined, making such effect more prominent. As a result, the computed SOC value for this molecule is ca. 1.54 cm^{-1}, the highest one among the molecules in this study.

DOI: 10.1021/jacs.6b12124
J. Am. Chem. Soc. 2017, 139, 4042−4051